Gibbs Ensemble Simulations of Vapor/Liquid Equilibrium Using the Flexible RWK2 Water Potential

Zhenhao Duan,[†,‡] Nancy Møller,[‡] and John H. Weare*[,‡]

Institute of Geology and Geophysics, Chinese Academy of Sciences, Beijing 100029, China, and Department of Chemistry, 0340, University of California, San Diego, La Jolla, California 92093

Received: December 19, 2003; In Final Form: June 17, 2004

Gibbs ensemble Monte Carlo simulations of water vapor/liquid equilibrium (VLE) using the flexible fixed charge RWK2 water−water potential are reported. The equilibrium densities, saturation pressures, and critical parameters calculated with this potential are in better agreement with experimental data than are values obtained from the SPC, MSPC/E, TIP4P, and TIP5P rigid fixed charge potentials as well as from polarizable interactions, such as those of the PPC, KJ, SPC/P, TIP4P/P, and SPCDP potentials. The agreement between predicted and experimental phase coexistence phase density versus temperature variation in the critical region is similar to that obtained from the SPC/E and the polarizable SPC-pol-1 potentials. However, the variation of the saturation pressure and heat of vaporization with temperature and the critical pressure predicted by the RWK2 potential are closer to experiment than predictions from SPC/E interaction and similar (for lower temperatures) to those of the MSPC/E potential. The water structure predictions of the RWK2 potential are substantially better than those from the SPC-pol-1 interaction. VLE data are not used to parametrize the RWK2 potential. Nevertheless, predictions for coexistence temperature versus phase density and saturation pressure versus temperature are similar to those of the recent potential of Errington and Panagiotopoulos (EP potential), which is adjusted to reproduce the VLE behavior of water. MD simulations using the RWK2 potential show much better agreement with the room-temperature liquid structure and second virial coefficient data than does the EP potential. Fixing the bond lengths and HOH angle in the RWK2 interaction at their isolated molecule minimum energy values leads to significant deterioration of the VLE predictions obtained.

Introduction

Knowledge of vapor/liquid-phase equilibria (VLE) of aqueous mixtures is important to the interpretation of many chemical, environmental, and geochemical processes. While there are excellent phenomenological models summarizing the extensive body of measurements of the thermodynamic behavior of pure water,[1] the experimental database available for water mixtures (e.g., H_2O-CO_2), which can show complex VLE behavior over large ranges of temperatures and pressures, is not sufficient to interpret many important processes. This problem is particularly severe for high TP conditions, where it is difficult to make accurate measurements. Applications requiring data for such conditions are commonly found in earth and planetary science.[2]

Molecular-level simulations of water mixtures could provide needed phase coexistence data in PTX regions where there are no measurements. However, the precision required to reliably interpret aqueous processes in many applications is high. Consequently, accurate descriptions of the intermolecular interactions in the mixture must be available for successful application of the simulation approach. For many aqueous mixtures, the water−water interactions are the most difficult to reproduce because of their hydrogen-bonding character. Since the VLE behavior of pure water is very well known, it is possible to test the accuracy of the description of the water−water interaction given by a potential by comparing molecular simulation results with this sizable database. Such validation is an important first step in developing simulation technology for the prediction of the properties of aqueous mixtures. Because the prediction of VLE behavior of mixtures is of great interest to the future application of this work, we emphasize in this Article realistic prediction of the critical properties and saturation pressure versus temperature behavior (i.e., the liquid/vapor line in the PT phase diagram) of pure water simulations.

VLE calculations are very demanding tests of the molecular-level description of a system, because they require that the simulated intensive variables (e.g., *T* and *P* or chemical potential of species) must be the same to high precision in the dense liquid phase as in the coexisting low-density vapor phase. The strong polar interactions required to describe the hydrogen-bonding structure of water make it difficult to develop interaction potentials that yield accurate simulations of the properties of water over this range of density. However, the intrinsic interest in water as a strongly polar fluid and its role as the principal component in many important mixtures have made the development of an efficient water−water potential for simulations an active area of research.

Many water−water potentials have been proposed. Most are based on the use of simple interactions (e.g., Lennard-Jones potentials) acting between molecular centers or between atoms on different molecules to describe attractive van der Waals and repulsive forces. Point charges placed near the centers of the atoms and positioned at fixed bond lengths and angles in the molecule are used to describe hydrogen-bonding behavior (herein these potentials are called rigid fixed charge potentials (RFCPs)). Examples of this class of potential are the SPC,[3] SPC/E,[4] MSPC/E,[5] TIP4P,[6] and TIP5P[7] potentials. Their descriptions

[†] Chinese Academy of Sciences.
[‡] University of California, San Diego.

10.1021/jp031338t CCC: $27.50
Published on Web 12/07/2004

TABLE 1: Critical Properties Predicted by Rigid Fixed Charge Water Potentials

potential	critical temperature (K)	critical pressure (bar)	critical density (g/cm^3)
SPC[a]	593.8	129	0.289
SPC/E[a]	638.6	139	0.295
MSPC/E[a]	609.8	139	0.310
EP[b]	645.9	183	0.297
TIP4P[c]	588.2	149.3	0.315
TIP5P[d]	521.3	85.6	0.336
RWK2[e]	649.0	243.0	0.297
Experimental	647.21	220.89	0.322

[a] Boulougouris et al.[5] [b] Errington and Panagiotopoulos.[9] [c] Lisal et al.[11] [d] Lisal et al.[12] [e] This study.

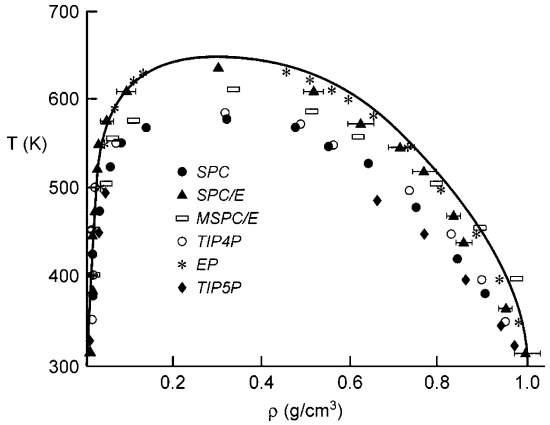

Figure 1. Comparison of coexisting vapor/liquid-phase densities vs temperature calculated using a selection of rigid fixed charge water−water potentials (symbols) with data[45] (solid line). The simulated results are taken from the references listed in the Table 1 footnotes.

of water−water interactions accurately reproduce many of the measured properties of water in the temperature and pressure region near that of the database used in their parametrization (e.g., $g_{OO}(r)$ and liquid density for temperatures near 298 K and pressures near 1 atm[8]). On the other hand, it has recently been shown[5] that most RFCPs lead to VLE predictions that are significantly in error, particularly as they approach the critical region. Because VLE properties are of great significance to interpretations of many important processes occurring in aqueous solutions, this is a significant limitation. Estimates of the reported critical temperature, pressure, and density properties predicted by RFCPs taken from the literature are summarized in Table 1. In Figure 1, the temperature versus phase density variation predictions from simulations using these potentials are compared with experimental data. With the exception of the SPC/E and EP potentials (discussed below), all of the predictions are unsatisfactory. While the VLE predictions from the SPC/E interaction are very good,[8] particularly in view of the simplicity of this potential, its predictions of the critical pressure (Table 1), saturation pressure versus temperature variation, and the second virial coefficient (see also Figure 10 and Figure 3 below) are not close to the measured values. Since one of our objectives is to use these potentials to make predictions of VLE behavior in mixed systems, it is important to have both the critical parameters and the saturation pressure of the pure water system well represented.

In an attempt to provide an RFCP that produces accurate predictions when compared to measured VLE properties, Errington and Panagiotopoulos parametrized a potential (the EP potential) to closely reproduce experimental coexisting vapor and liquid densities, saturation pressures and critical parameters

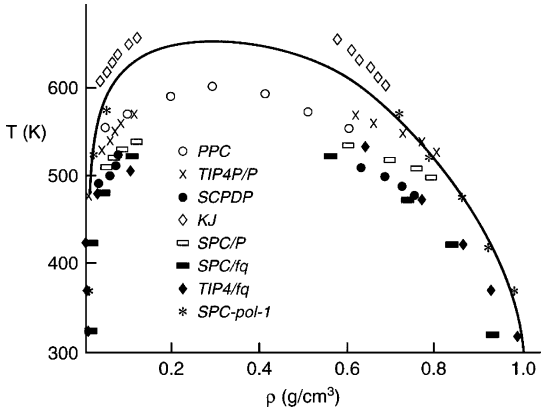

Figure 2. Comparison of coexisting vapor/liquid-phase densities vs temperature calculated using a selection of polarizable water−water potentials (symbols) with data[45] (solid line). The simulated results are taken from the references listed in the Table 2 footnotes.

using the Hamiltonian scaling method.[9] Predictions from the EP potential provide good agreement with phase coexistence, saturation pressure, and phase density versus pressure data (see Figure 1 and Table 1). However, the structural properties of the liquid state (e.g., the radial distribution functions) are not satisfactory. The second shell peak in $g_{OO}(r)$, which is well resolved in the scattering data,[8,10] is not resolved in the simulated radial distribution function.[9]

A possible source of error in these RFCP potentials is the lack of a mechanism to incorporate the effects on the charge distribution within a water molecule caused by the local electric field change with a change in density of the surrounding water (polarization). This problem has been discussed extensively in the literature.[13−19] The dipole moment of water varies from 1.855 D in the low-density vapor state to 2.4−2.6 D[20] in the high-density liquid state. Therefore, changes in the charge distribution in water molecules occur that can significantly affect observed properties.

Recently, a number of water−water interaction potentials have been reported that include the effect of polarization of the water molecules phenomenologically (herein called polarizeable potentials (PPs)). Examples of PPs include the SPC-FQ,[21] SPC/P,[18] TIP4P/P,[18] TIP4P−FQ,[13] SCPDP,[16] KJ,[22] PPC,[17] and SPC-pol-1[15] interactions. Unfortunately, as has been discussed by others,[14,19] these PPs do not provide a significant improvement in the prediction of VLE behavior. The predicted pressure versus density variations from recently reported PPs are given in Figure 2. The critical temperature, pressure, and density properties predicted by these potentials are summarized in Table 2. With the exception of the SPC-pol-1 interaction, which is parametrized to give agreement with VLE data, none of these potentials gives a satisfactory description of VLE behavior. The SPC-pol-1 potential gives reasonable predictions, as shown in Figure 2. However, as with the EP interaction, MD simulations using this PP lead to a very poor description of the H-bonding structure in the liquid state (i.e., the predicted $g_{OO}(r)$ does not show the experimentally well resolved peak corresponding to the second solvation shell[15]).

In this article, Gibbs ensemble Monte Carlo[23] (GEMC) calculations of VLE properties for water are reported using a water−water potential developed by Watts and co-workers.[24−27] This potential has received relatively little attention in the literature. However, simulations using this interaction, which is parametrized primarily from gas- and solid-phase data, predict many properties of ice, water vapor, and liquid water quite accurately.[24−28] We show in the following that, using this

TABLE 2: Critical Properties Predicted by Polarizable or Fluctuating Charge Water Potentials

model	critical temperature (K)	critical pressure (bar)	critical density (g/cm^3)
SPC/P[a]	551	156[e]	0.34
TIP4P/P[a]	587	148[e]	0.35
SCPDP[a]	538	100[e]	0.32
SPC/FQ[b]	540		0.33
TIP4P/FQ[b]	570		0.35
PPC[c]	606	195	0.30
SPC-pol-1[d]	650		
KJ[a]	685	278	0.32
experimental	647.21	220.89	0.322

[a] Kiyohara et al.[18] [b] Chen et al.[21] [c] Hayward and Svishchev.[19] [d] Chen et al.[15] [e] The simulated pressures are approximate estimations from the figures in the references.

potential, VLE predictions are remarkably reliable even for temperatures near the critical value, which is far away from the region of parametrization.

RWK2 Water−Water Potential

The RWK2 potential is defined in detail in the Appendix and discussed in several references.[24−28] It is a flexible fixed charge potential (changes of bond length and angle possible) with intramolecular interactions consisting of atom−atom Morse potentials plus an additional local coordinate coupling term. These intramolecular contributions have been adjusted to fit the rotational and vibrational spectrum of the gas-phase water molecule.[24−27] The intermolecular interactions include Coulomb interactions between charges placed on the hydrogen atoms and near the oxygen atoms of the molecule pairs. The charges on the water molecules have been adjusted to reproduce the dipole and quadrapole moments of an isolated water molecule. Intermolecular site interactions between the hydrogen atoms on different molecules are given by exponential repulsive interactions. Interactions between the oxygen and hydrogen atoms on different molecules are given by Morse potentials. The intermolecular oxygen−oxygen interaction is represented by an exponential repulsive potential plus an attractive damped dispersion form[29] known to produce highly accurate long-range atomic interactions in the gas phase. The parameters for the intermolecular contributions to the potential are evaluated from data for the second virial coefficient and the static lattice energies of ices Ih, VII, and VIII. No liquid-state data are used in the parametrization. The prediction of a number of properties of water and ice are discussed in the previously cited references introducing the RWK2 potential.[24−28]

To calculate vapor/liquid coexistence, the properties of both the liquid and the gas phases must be predicted accurately for the temperature and pressure ranges of interest. The PVT properties for the low-density phase can be calculated from the density virial expansion,[30] retaining only the term linear in density. The coefficient of this term is the second virial coefficient. Our numerically calculated values of this coefficient using the SPC/E, TIP4P, EP, and RWK2 potentials are compared with measured second virial coefficient measurements for water[31] in Figure 3. The values given by the RWK2 potential agree better with the data than those given by the other three interaction potentials. This is expected because the second virial coefficient is used in the parametrization of this potential.[25] We note that the SPC/E potential, which gives quite good VLE predictions, does not produce a good estimate of the second virial coefficient.

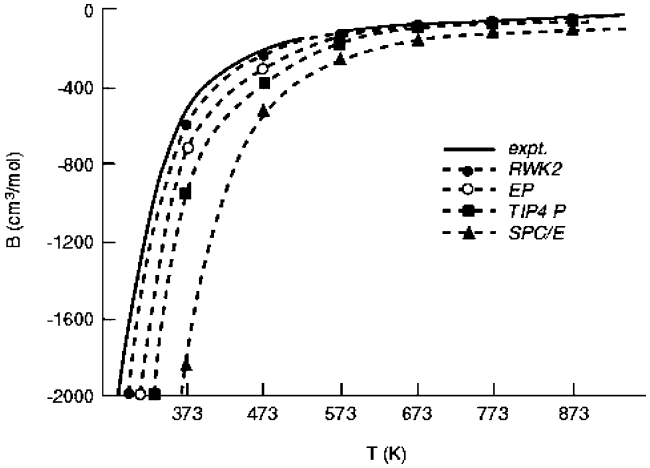

Figure 3. Comparison of numerically calculated second virial coefficients for water using the RWK2 potential with experimental data[31] (solid line) and with our calculations using other potential interactions.

The PVT behavior of water predicted from molecular dynamics (MD) simulations using this potential have been compared with experimental data for wide ranges of temperature and pressure in Duan et al.[28] Calculations agree with density data within 1−5% from 5 to 10 000 bar and from 300 to 1600 K. This agreement is similar to that found with the TIP4P water−water potential.[32]

More detailed information about the quality of the description of the liquid state can be obtained from a comparison of simulated radial distribution functions with the distributions obtained from scattering experiments. Our MD simulations included 256 water molecules. Periodic boundary conditions and minimum image conventions were used to treat out-of-box atoms and to calculate interatom distances with a potential cutoff for short-range forces at half of the simulation box length. Long-range electrostatic forces and energies were calculated using the Ewald summation procedure.[33] The screening parameter is 5.0, and 1000 reciprocal lattice vectors were used to compute the reciprocal space sum. The time step for all simulations was 0.75 fs. Energy and momentum conservation was checked during the trajectory. After a 10-ps preequilibration simulation, the instantaneous configurations (for ∼20 ps) were used to compute the average behavior.

Although the RWK2 potential is not parametrized from any liquid data, its predictions of the structural properties of liquid water are quite good. Soper[10] and Sorensen et al.[8] recently reevaluated water scattering data and revised the oxygen−oxygen radial distribution function, $g_{OO}(r)$, for 298 K and 1 g/cm^{3}density. The $g_{OO}(r)$s from both these reevaluations are essentially the same. As shown in Figure 4, the $g_{OO}(r)$ computed from our MD simulations using the RWK2 potential agrees well with these new $g_{OO}(r)$s. (For a comparison of the experimentally derived $g_{OO}(r)$ with the results of MD simulations using other potentials, see Sorensen et al.[8]) The higher value of the minimum after the first peak in Figure 4 suggests that the RWK2 potential may produce slightly understructured results. The hydrogen−hydrogen, $g_{HH}(r)$, and oxygen−hydrogen, $g_{OH}(r)$, radial distribution functions for liquid water at 298 K and 1 g/cm^3 calculated using the RWK2 potential are compared with those of Soper and Phillips[34] in Figure 5. The agreement of the peak positions for $g_{HH}(r)$ is good. Agreement with the $g_{OH}(r)$ data is not as satisfactory. The results of recent ab initio molecular dynamics

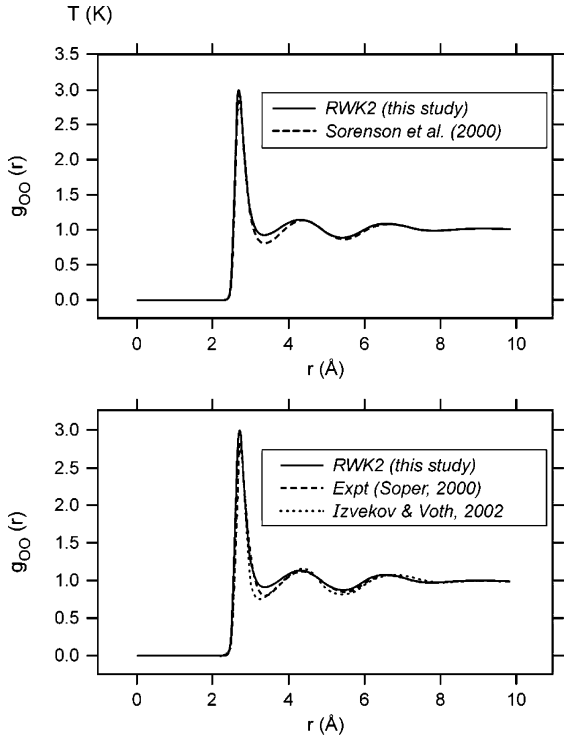

Figure 4. Comparison of calculated oxygen−oxygen radial distribution functions, $g_{OO}(r)$, for water at 298 K and 1.0 g/cm^3 using the RWK2 potential with recent experimental data[8,10] and recent AIMD results.[35]

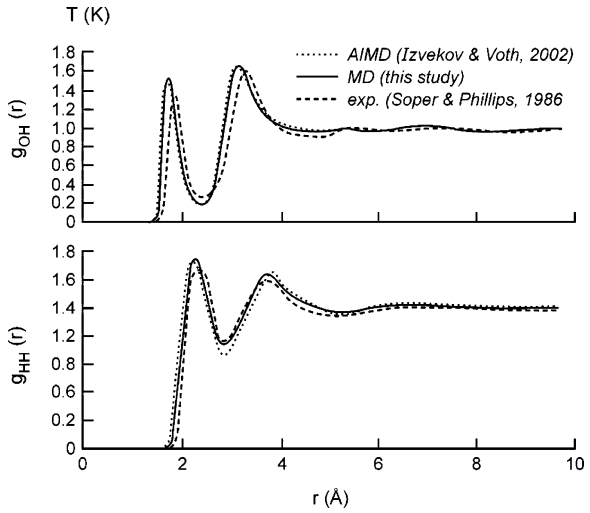

Figure 5. Comparison of calculated hydrogen−hydrogen, $g_{HH}(r)$, and oxygen−hydrogen, $g_{OH}(r)$, radial distribution functions for water at 298 K and 1.0 g/cm^3 using the RWK2 potential with experimental data[34] and recent AIMD results.[35]

(AIMD) simulations[35] are also included in Figures 4 and 5. The agreement of these calculations with the observed radial distributions is similar in overall accuracy to that given by the RWK2 potential. The results reported in Figures 4 and 5 using the RWK2 potential are similar to MD results using the SPC/E potential[10,36] for $g_{OH}(r)$ and $g_{HH}(r)$. However, simulation with the SPC/E potential produces a very accurate $g_{OO}(r)$.[8]

Experimental radial distribution function data[37] and AIMD simulations[38] for water have also been reported for higher temperature (T = 653 K) and density (0.73 g/cm^3). The distribution functions derived from our MD simulations using the RWK2 potential for these conditions are compared with the experimental data and the AIMD simulation results in Figure 6. At this temperature, the RWK2 potential seems to produce

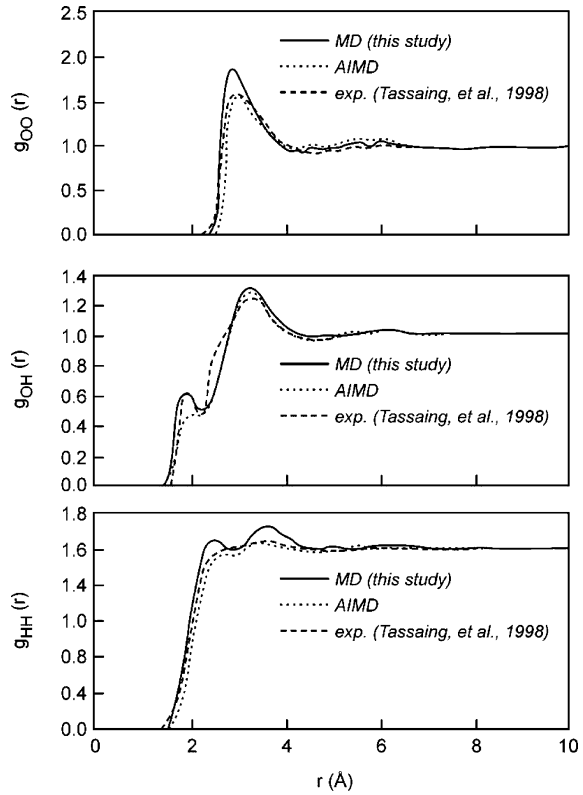

Figure 6. Comparison of calculated radial distribution functions of water at 653 K. and 0.73 g/cm^3 using the RWK2 potential with experimental data[37] and AIMD simulations.[38]

overstructured results; i.e., the maximum in our calculated $g_{OO}(r)$ function is larger than that of the experimental data. However, this maximum value is about the same as the maximum in the data taken at a slightly higher temperature (673 K and 0.73 g/cm^3) by Soper et al.[39] The agreement of AIMD simulations with the experimental data for $g_{OH}(r)$, and $g_{HH}(r)$ is slightly better than that of the RWK2 calculations for these conditions. Because of the large system size and large number of steps required (see below), it is not possible to use first principles methods to predict VLE.

Gibbs Ensemble Simulation Of Vapor/Liquid-Phase Equilibria

The Gibbs ensemble Monte Carlo method[23] appears to be the most efficient method to simulate vapor/liquid-phase coexistence. Here, we report GEMC calculations of the VLE properties of water using the RWK2 potential for temperatures up to the critical temperature of water. These NVT Monte Carlo simulations were carried out in two cells. A total of 512 water molecules were distributed between the two boxes. The Coulomb potential energy was calculated using an Ewald sum with the same parameters as in the MD simulations discussed above. All the intersite distances were evaluated using the minimum image convention.[33]

The total number of water molecules, total volume of the two simulation boxes, and the temperature were held constant throughout the simulation. The initial structures for the liquid and the vapor were taken either from previous GEMC simulated configurations or from MD results with a TIP4P-like potential, which had the same geometry as a rigid RWK2 potential with bond lengths and angles fixed at the lowest energy structure for an isolated molecule. The simulation cycles began with 512 or 1024 (for low temperatures) attempted molecule displace-

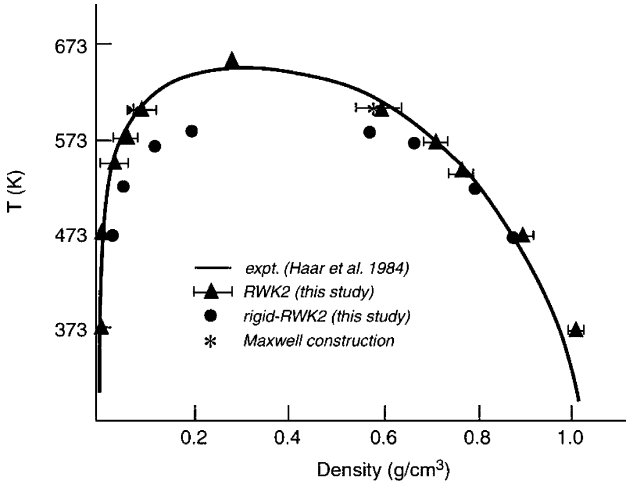

Figure 7. Comparison of coexisting vapor/liquid-phase densities vs temperature for water calculations using the flexible RWK2 potential or the rigid RWK2 potential (see text) with experimental data.[45] The asterisks (for $T = 600$ K) indicate results of MD simulation and a Maxwell construction as in Figure 8.

ments within the phases, followed by 1 attempted volume change and 2−40 attempted molecule exchanges between phases. Each molecule displacement consisted of the following steps: (1) random displacement of the oxygen atom in Cartesian coordinates (δx, δy, δz), (2) displacement of the hydrogen atoms by the same distance as the oxygen atom (δx, δy, δz), (3) displacement of the hydrogen atoms by random Cartesian coordinate displacements with the condition that the HOH angle after the displacement was between 97° and 114° and that the OH bond length was within 1.71−1.96 au. These values are based on the statistics of our previous molecular dynamics studies using the RWK2 potential. The number of attempted displacements and attempted particle exchanges required to reach equilibrium depended on the temperature. For higher temperatures, fewer were needed to equilibrate. For temperatures near the critical temperature, 512 attempted molecular displacements and 2−3 attempted particle exchanges were sufficient in each cycle. Normally, 20 000−100 000 cycles were needed to achieve the 10 000−50 000 successful insertions that were sufficient to obtain statistically significant averages. If the initial state was not far from equilibrium, only 10 000 successful exchanges were required to equilibrate the system. At 573 K, different initial states were used to ensure that the simulation was not trapped in a local equilibrium state. All these simulations led to essentially the same final average configuration.

A major difficulty in implementing the GEMC method is the low acceptance ratio of molecular insertion into the liquid phase, especially at high densities. To enhance the likelihood of successful insertions, we tried both the inflating flea method[40] and the rotation insertion bias method.[41] The inflating flea method improves the insertion acceptance in the high-temperature range. However, for lower temperatures ($T < 473$ K), the very low solubility of the "flea" made this method ineffective, because too few "flea" molecules could be dissolved in the liquid. In the rotation insertion bias method, the molecule is moved after insertion in such a way that its dipole moment rotates around its oxygen center in an effort to find an accepted configuration. Using this method, the acceptance ratio was increased by 5−6-fold relative to an equal-probability random insertion.

In Figure 7, the densities of the coexisting vapor and liquid phases as a function of temperature simulated using the RWK2 potential are compared with experimental results. For the vapor side, which are difficult to read from Figure 7, the density from the RWK2 potential simulations at 373 K is ∼23% higher than the experimental value. This value seems high. However, we note that water vapor density predictions using GEMC simulations typically have large errors when compared to experimental measurements. For example the vapor density predicted by the SPC/E potential is 53% larger for $T = 389$ K.[5] To provide a further check on the convergence of the GEMC calculations, we calculated the VLE at 600 K using constant-temperature MD simulations and a Maxwell construction[42] (see Figure 8). These calculations yield VLE that are consistent with our GEMC simulations (see asterisks in Figure 7).

To estimate the density and temperature coordinates of the critical point predicted using the RWK2 potential, the coefficients of the truncated Wegner expansion[43] were adjusted to fit the difference between simulated densities of the coexisting phases at 610, 600, and 573 K. When truncated after the second term, the Wegner expansion is

$$|\rho_l - \rho_v| = A_1(T_c - T)^{\beta} + A_2(T_c - T)^{\beta/2} \qquad (1)$$

where $\beta = 0.325$. This procedure gave an estimated critical temperature of 649 K, which compares well with the experimental value of 647.25 K. The critical density was calculated to be 0.297 g/cm^3 by fitting the density to the law of rectilinear diameter,[44]

$$(\rho_l + \rho_v)/2 = \rho_c + B(T - T_c) \qquad (2)$$

This compares reasonably well with the experimental value[45] of 0.322 g/cm^3 (see Tables 1 and 2). The critical pressure was estimated by fitting our saturationr pressure versus temperature data ($T < 610$ K) to the Antoine equation[11,46] and extrapolating to the critical temperature. This leads to an estimated critical pressure of 243 bar. The experimental value is 220.89 bar.[45]

As shown in Figure 9, the simulated enthalpy of vaporization using the RWK2 potential deviates from the steam table data[45] by less than 1.5 kJ/mol, which is close to the experimental accuracy. These results are substantially better than those obtained from the SPC/E potential (see Figure 9). The RWK2 potential also produces accurate saturation pressure predictions (see Figure 10). Results using the SPC/E potential are not satisfactory. However, a modification of the SPC/E potential, the MSPC/E[5] potential, produces results that are similar to the RWK2 potential.

Because of the additional internal degrees of freedom, it takes roughly 1.5 times longer to equilibrate the flexible RWK2 potential as compared to a rigid potential. Therefore, we investigated how well simulations using a rigid RWK2 potential (bond lengths and angles fixed to give the lowest intramolecular potential energy for an isolated molecule) agree with VLE data. The results from these GEMC simulations are included in Figure 7. Simulations with the rigid potential yield vapor densities 30−120% higher than the measured densities in the coexistence region. Furthermore, the predicted critical temperature and pressure using the rigid potential are well below the measured values ($T_c = 581$ K and $P_c = 140$ bar for the rigid potential versus the experimental values of 647.26 K and 220.89 bar). These results are similar to those reported for the TIP4P potential.[11]

Conclusions

Molecular simulations of the thermodynamic properties of aqueous mixtures have many important applications to problems in industrial chemistry, environmental chemistry, and earth

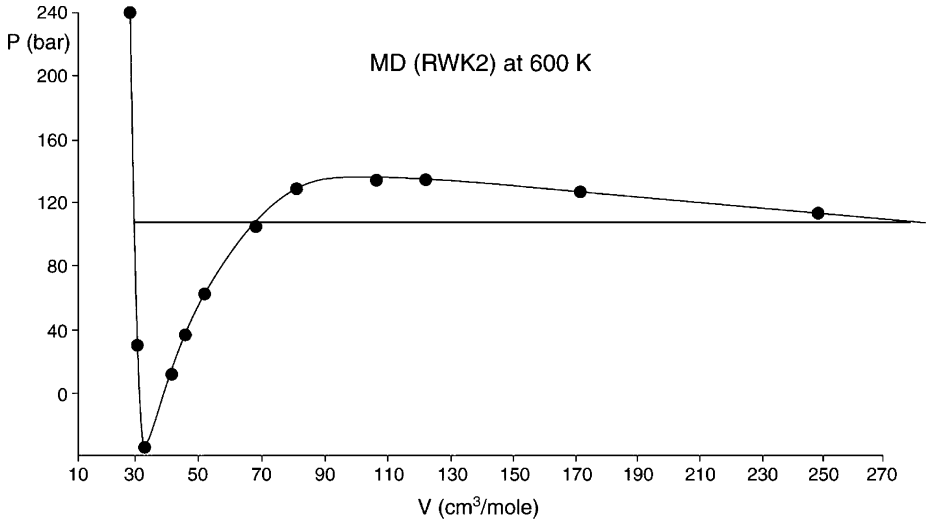

Figure 8. Calculatedf vapor/liquid coexistence at 600 K using MD, the RWK2 potential and a Maxwell construction. Liquid density 28.4 cm^3/mol and vapor density 277 cm^3/mol vs 28.0 and 246 cm^3/mol found using GEMC simulations as in Figure 7.

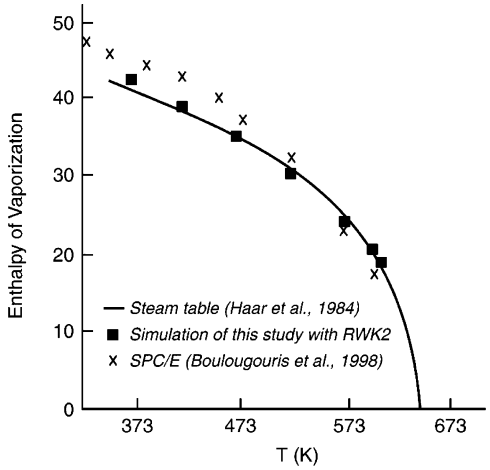

Figure 9. Comparison of enthalpy of vaporization for water calculated using the RWK2 potential or SPC/E potential interactions with data.[45]

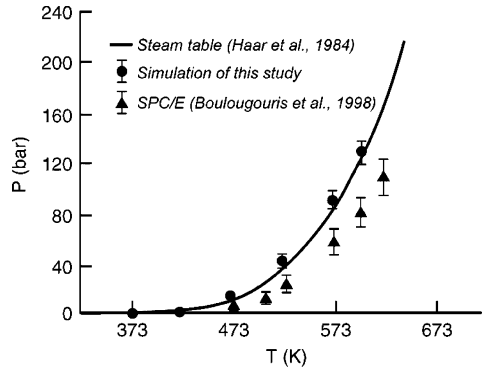

Figure 10. Comparison of water saturation pressure estimations using the RWK2 potential or the SPC/E potential with data.[45]

science. The recent significant decrease in the cost/performance ratio of computers has made the implementation of such technology possible from the algorithm and computer-time point of view. The limitation to developing this technology is the availability of effective intermolecular potentials for simulation use that can provide thermodynamic information with sufficient accuracy for use in these applications.

In this article, we test the ability of the flexible RWK2 potential, developed by Watts and co-workers,[24−27] to successfully describe water−water interactions in simulations of a variety of pure water properties with emphasis on vapor/liquid equilibrium. Three criteria that a pure water simulation model must meet in order to achieve our objective of successfully predicting VLE in aqueous mixtures are as follows: (1) The pure water system vapor/liquid line should be well predicted to the critical temperature of water in order to have a correct PT projection in the binary; (2) the coexisting phase densities in the pure system must be correctly predicted; (3) the description of the H-bonding structure of water should be well represented. We find that of the many potentials for which VLE predictions are available, four (SPC/E, RWK2, EP, SPC-pol-1) produce successful predictions of water VLE. The EP and SPC-pol-1 potentials are eliminated because of their poor description of the liquid-phase structure, although they both produce acceptable predictions of the heat of vaporization and vapor pressure as a function of temperature. The SPC/E and RWK2 potentials give similar predictions of the density of the liquid phase versus temperature and the critical temperature and density (Table 1). However, the SPC/E results for critical pressure (Table 1), saturation pressure versus temperature (Figure 10), and enthalpy of vaporization versus temperature (Figure 9) are considerably less accurate than those using the RWK2 potential. These predictions can be improved by using the similar MSPC/E potential.[5] However, the critical temperature and, therefore, the critical pressure predicted from this model are not satisfactory (Table 2).

Because the dipole moment of the RWK2 is fixed at the gas-phase value, predictions of dielectric constants of water (our MD calculations, simulation parameters as above) at ambient temperatures are low, which is a limitation of this model. However, at critical temperatures, the dielectric constant is within 20% of the measured value. In addition, using the RWK2 potential in an MD simulation leads to a simulated liquid density 5% larger than the experimental values for $T = 298$ K and 1 bar. This is not as good as that produced by some RFCP. For example, the liquid density predicted by the SPC/E interaction is 2% smaller than the measured value at this temperature and pressure. Nevertheless, the accurate results using the RWK2 potential for critical pressure, vapor pressure versus temperature, and enthalpy of vaporization lead us to believe that the RWK2 potential is a promising candidate for predicting aqueous mixture VLE at temperatures and pressures near and above the critical temperature.

Appendix: RWK2 Potential

The RWK2 potential is a pairwise-additive interaction that includes both intramolecular and intermolecular terms. This potential is presented in a series of papers by Watts and coworkers.[24−27] The final version used in the simulations presented here appears in Coker and Watts.[27] In this interaction potential, two hydrogen nuclei are located at positions R_1 and R_2; each of these carries a positive charge q. A negative charge, $-2q$, is located at position $R_0 = R_2 + (R_{H1} + R_{H2} - 2R_0)\delta$. The position of the negative charge changes as the geometry of the water molecule changes, which, in turn, changes according to the molecular environment.

$$V_{\text{int } ra} = \sum_{i=1}^{3} D_i(1 - e^{-\alpha s_i})^2 + f_{12}s_1s_2 \qquad \text{(A1)}$$

The intramolecular term consists of atom−atom potentials,

$$s_i = r_{OHi}\cos\left(\frac{\theta - \theta_0}{2}\right) - R_0, \quad i = 1, 2 \qquad \text{(A2)}$$

where the local modes are defined as

$$s_3 = \frac{r_{OH_1} + r_{OH_2}}{R_0}\sin\left(\frac{\theta - \theta_0}{2}\right) \qquad \text{(A3)}$$

The intermolecular term has the form

$$V_{\text{inter}} = \sum_{i,j}^{3}\frac{q_iq_j}{r_{ij}} + \sum_{O,O}A_{OO}e^{-\alpha_{OO}r_{OO}} + \sum_{H,H}A_{HH}e^{-\alpha_{HH}r_{HH}} + \sum_{O,H}A_{OH}e^{-\alpha_{OH}(r_{OH}-r_0)}[e^{-\alpha_{OH}(r_{OH}-r_0)} - 2] + \sum_{O,O}\left\{-f\left[C_6\left(\frac{g_6}{r_{OO}}\right)^6 + C_8\left(\frac{g_8}{r_{OO}}\right)^8 + C_{10}\left(\frac{g_{10}}{r_{OO}}\right)^{10}\right]\right\} \qquad \text{(A4)}$$

The first term in eq A4 represents the Coulomb interactions. The second and third terms are the short-range exponential repulsion for hydrogen−hydrogen and oxygen−hydrogen interactions, respectively. The fourth term is a Morse potential for oxygen−hydrogen interactions. The final term is a molecular dispersion term,[29] which is a function of oxygen−oxygen distances. The function f in the last term is given by

$$f = 1 - (cr_{OO})^{\beta}e^{-cr_{OO}} \qquad \text{(A5)}$$

and g_n by

$$g_n = 1 - e^{-(ar_{OO}/n + br^2_{OO})/(n)_2} \qquad \text{(A6)}$$

All the parameters are listed in the Appendix of Duan et al.[28]

Acknowledgment. The support of the following grants is acknowledged: NSF EAR-0126331, DOE DE-FG02-02ER15311, DOE-FG36-99ID13745, and ACSPRF37196AC9.

References and Notes

(1) Wagner, W.; Pruss, A. *J. Phys. Chem. Ref. Data* **2002**, *31*, 387.

(2) Roedder, E. Fluid inclusions. In *Reviews in Mineralogy*; Mineralogical Society of America: Washington, DC, 1984; Vol. 12.

(3) Berendsen, H. J. C.; Postma, J. P. M.; van Gunsteren, W. F.; Hermans, J. In *Intermolecular forces*; Pullman, B., Ed.; D. Reidel Publishing Co.: Dordrecht, The Netherlands, 1981; p 331.

(4) Berendsen, H. J. C.; Grigera, J. R.; Straatsma, T. P. *J. Phys. Chem.* **1987**, *91*, 6269.

(5) Boulougouris, G. C.; Economou, I. G.; Theodorou, D. N. *J. Phys. Chem. B* **1998**, *102*, 1029.

(6) Jorgensen, W. L. *J. Chem. Phys.* **1982**, *77*, 4156.

(7) Mahoney, M. W.; Jorgenson, W. L. *J. Chem. Phys.* **2000**, *112*, 8910.

(8) Sorenson, J. M.; Hura, G.; Glaeser, R. M.; Head-Gordon, T. *J. Chem. Phys.* **2000**, *113*, 9149.

(9) Errington, J. R.; Panagiotopoulos, A. Z. *J. Phys. Chem. B* **1998**, *102*, 7470.

(10) Soper, A. K. *Chem. Phys.* **2000**, *258*, 121.

(11) Lisal, M.; Smith, W. R.; Nezbeda, I. *Fluid Phase Equilib.* **2001**, *181*, 127.

(12) Lisal, M.; Kolafa, J.; Nezbeda, I. *J. Chem. Phys.* **2002**, *117*, 8892.

(13) Rick, S. W.; Stuart, S. J.; Berne, B. J. *J. Chem. Phys.* **1994**, *101*, 6141.

(14) Rivera, J. L.; Predota, M.; Chialvo, A. A.; Cummings, P. T. *Chem. Phys. Lett.* **2002**, *357*, 189.

(15) Chen, B.; Xing, J. H.; Siepmann, J. I. *J. Phys. Chem. B* **2000**, *104*, 2391.

(16) Chialvo, A. A.; Cummings, P. T. *J. Chem. Phys.* **1996**, *105*, 8274.

(17) Svishchev, I. M.; Kusalik, P. G.; Wang, J.; Boyd, R. J. *J. Chem. Phys.* **1996**, *105*, 4742.

(18) Kiyohara, K.; Gubbins, K. E.; Panagiotopoulos, A. Z. *Mol. Phys.* **1998**, *94*, 803.

(19) Hayward, T. M.; Svishchev, I. M. *Fluid Phase Equilib.* **2001**, *182*, 65.

(20) Gregory, J. K.; Clary, D. C.; Liu, K.; Brown, M. G.; Saykally, R. J. *Science* **1997**, *275*, 814.

(21) Chen, B.; Potoff, J. J.; Siepmann, J. I. *J. Phys. Chem. B* **2000**, *104*, 2378.

(22) Kozack, R. E.; Jordan, P. C. *J. Chem. Phys.* **1992**, *96*, 3120.

(23) Panagiotopoulos, A. Z. *Mol. Phys.* **1987**, *61*, 813.

(24) Watts, R. O. *Chem. Phys.* **1977**, *26*, 367.

(25) Reimers, J. R.; Watts, R. O.; Klein, M. L. *Chem. Phys.* **1982**, *64*, 95.

(26) Reimers, J. R.; Watts, R. O. *Chem. Phys.* **1984**, *91*, 201.

(27) Coker, D. F.; Watts, R. O. *J. Phys. Chem.* **1987**, *91*, 2513.

(28) Duan, Z. H.; Moller, N.; Weare, J. H. *Geochim. Cosmochim. Acta* **1995**, *59*, 3273.

(29) Douketis, C.; Scoles, G.; Marchetti, S.; Zen, M.; Thakkar, A. J. *J. Chem. Phys.* **1982**, *76*, 3057.

(30) Sandler, S. I. *Chemical and Engineering Thermodynamics*, 3rd ed.; John Wiley & Sons: New York, 1999.

(31) Tsonopoulos, C.; Heidman, J. L. *Fluid Phase Equilib.* **1990**, *57*, 261.

(32) Brodholt, J.; Wood, B. *Geochim. Cosmochim. Acta* **1990**, *54*, 2611.

(33) Allen, M. P.; Tildesley, D. J. *Computer simulation of liquids*; Clarendon Press/Oxford University Press: Oxford England, 1987.

(34) Soper, A. K.; Phillips, M. G. *Chem. Phys.* **1986**, *107*, 47.

(35) Izvekov, S.; Voth, G. A. *J. Chem. Phys.* **2002**, *116*, 10372.

(36) Watanabe, K.; Klein, M. L. *Chem. Phys.* **1989**, *131*, 157.

(37) Tassaing, T.; Bellissent-Funel, M. C.; Guillot, B.; Guissani, Y. *Europhys. Lett.* **1998**, *42*, 265.

(38) Boero, M.; Terakura, K.; Ikeshoji, T.; Liew, C. C.; Parrinello, M. *Phys. Rev. Lett.* **2000**, *85*, 3245.

(39) Soper, A. K.; Bruni, F.; Ricci, M. A. *J. Chem. Phys.* **1997**, *106*, 247.

(40) de Pablo, J. J.; Prausnitz, J. M. *Fluid Phase Equilib.* **1989**, *53*, 177.

(41) Cracknell, R. F.; Nicholson, D.; Parsonage, N. G.; Evans, H. *Mol. Phys.* **1990**, *71*, 931.

(42) Berry, R. S.; Rice, S. A.; Ross, J. *Physical Chemistry*; John Wiley & Sons: New York, 1980.

(43) Wegner, F. J. *Phys. Rev. B* **1972**, *5*, 4529.

(44) Ley-Koo, M.; Green, M. S. *Phys. Rev. A* **1981**, *23*, 2650.

(45) Haar, L.; Gallagher, J. S.; Kell, G. S. *Steam Table*; Hemisphere Publishing Corp.: Washington, DC, 1984.

(46) Poling, B. E.; Prausnitz, J. M.; O'Connell, J. P. *The properties of gases and liquids*, 5th ed.; McGraw-Hill: New York, 2001.